ELSEVIER

Biophysical Chemistry 99 (2002) 143–154

Biophysical Chemistry

www.elsevier.com/locate/bpc

# Analysis of resonance energy transfer in model membranes: role of orientational effects

Yegor A. Domanov, Galina P. Gorbenko*

*V.N. Karazin Kharkiv National University, 4 Svobody sq., Kharkiv 61077, Ukraine*

Received 16 April 2002; received in revised form 22 May 2002; accepted 27 May 2002

**Abstract**

The model of resonance energy transfer (RET) in membrane systems containing donors randomly distributed over two parallel planes separated by fixed distance and acceptors confined to a single plane is presented. Factors determining energy transfer rate are considered with special attention being given to the contribution from orientational heterogeneity of the donor emission and acceptor absorption transition dipoles. Analysis of simulated data suggests that RET in membranes, as compared to intramolecular energy transfer, is substantially less sensitive to the degree of reorientational freedom of chromophores due to averaging over multiple donor-acceptor pairs. The uncertainties in the distance estimation resulting from the unknown mutual orientation of the donor and acceptor are analyzed.


*Keywords:* Resonance energy transfer; Distance estimation in membrane; Orientation factor

## 1. Introduction

Structure–function relationships in biological membranes are known to be governed by a variety of factors depending on the spatial and orientational organization of the protein–lipid assemblies [1,2]. The problem of structural characterization of these assemblies has been approached by a number of physical methods including X-ray and neutron diffraction [3,4], NMR [5–8], ESR [9], IR and fluorescence spectroscopy [10–19], etc. In ascertaining the transverse protein location in a lipid bilayer, spectroscopic techniques based on non-resonance (collisional) [16,20] or resonance (energy-transfer) [10,21,22] fluorescence quenching are believed to be particularly well-suited.

The efficiency of resonance energy transfer (RET) is a function of the distance between the chromophores employed as energy donor and acceptor, the donor quantum yield, overlap of the donor emission and acceptor absorption spectra and relative orientation of the donor and acceptor transition dipoles [10]. Importantly, the character of this function strongly depends on the geometry and dimensionality of the system being examined [10,23]. Specifically, adequate description of RET in membranes requires the application of particular theoretical models developed for analyzing energy transfer in two-dimensional systems [24,25]. Theo-

*Corresponding author. 52-52 Tobolskaya street, Kharkiv 61072, Ukraine.

*E-mail address:* galyagor@yahoo.com (G.P. Gorbenko).

0301-4622/02/$ - see front matter 
PII: S0301-4622(02)00143-6

retical analyses clearly indicate that such factors as the mode of acceptor bilayer distribution, the curvature of lipid–water interface, the extent of area exclusion around fluorophore, etc. could significantly contribute to the RET efficiency [25–29]. Another essential contribution that is regarded as the main source of uncertainty in the quantitative interpretation of RET data is determined by the chromophore relative orientation affecting the value of such parameter as the orientation factor. This limitation of the RET method has long been a focus of numerous theoretical considerations, and a number of approaches have been proposed to circumvent the problem of orientation factor [30–33]. In the context of membrane studies, this problem acquires some new facets that are worth special analysis.

The present study has been undertaken to assess the role of orientational effects in determining the rate of energy transfer in membrane systems. The RET model proposed previously for two-dimensional systems [25] has been extended here to the case of chromophore distribution over three parallel planes—one acceptor-containing and two donor-containing ones. Analysis of simulated data has revealed the possibility of minimizing the uncertainty in the RET-based distance estimation by selecting donor–acceptor pairs with appropriate parameters.

## 2. Theory

### 2.1. General formalism

To treat the problem of energy transfer in two-dimensional membrane systems many theoretical approaches, differing in their complexity, have been developed [24–29]. One of them, proposed by Wolber and Hudson [25], has been extended here to the case of donors uniformly distributed between the outside and inside of the bilayer and acceptors confined to one membrane leaflet (Fig. 1). The formalism employed in derivation of the expression for the relative quantum yield of a donor can be briefly described as follows.

The rate constant of energy transfer by Förster mechanism (in the limit of weak dipole–dipole coupling) is a function of excited donor lifetime

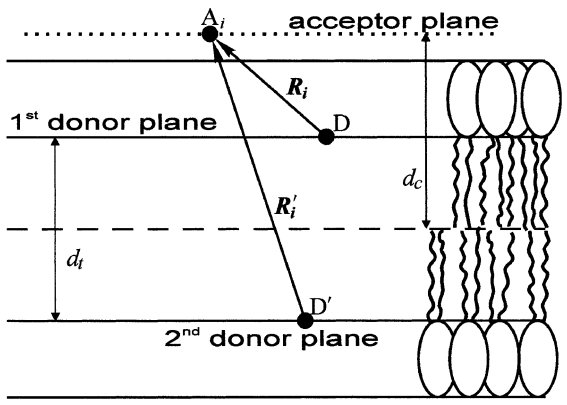


Fig. 1. Schematic for disposition of donor and acceptor planes within the bilayer as assumed in the model. The donor molecule D (or D′) is surrounded by an array of adjacent acceptors $A_i$ (only one acceptor molecule is shown for clarity).

in the absence of acceptos $\tau_D$, Förster radius $R_0$, and distances between a given donor and the $i$th acceptor in its surroundings $\{R_i\}$:

$$k_T = \tau_D^{-1} \sum_{i=1}^{N} (R_0/R_i)^6, \quad (1)$$

where $N$ is the number of acceptor molecules within the sphere of radius $R_d$ (centered at the donor molecule) beyond which there is no energy transfer. Since at low surface density of a donor the rate of energy transfer is independent of its concentration, one needs only consider a system consisting of one donor molecule and a set of acceptors with $R_i \leqslant R_d$ (or rather an ensemble of such systems with different $\{R_i\}$).

The probability that a donor excited at the moment $t_0 = 0$ will remain excited after time $t$ is described by the first-order kinetic equation:

$$-\frac{dP(t)}{dt} = (k_T + \tau_D^{-1})P(t) = \tau_D^{-1}\left(1 + \sum_{i=1}^{N} (R_0/R_i)^6\right)P(t). \quad (2)$$

After integration with the initial condition $P(0) = 1$ one obtains:

$$P(t) = \exp(-t/\tau_D) \prod_{i=1}^{N} \exp[(-t/\tau_D)(R_0/R_i)^6]. \quad (3)$$

Ensemble averaged fluorescence decay function $\langle P(t)\rangle$ can be written as [25]:

$$\langle P(t)\rangle = \exp(-t/\tau_D)\prod_{i=1}^{N}\int_0^{R_d}\exp\left[(-t/\tau_D)(R_0/R_i)^6\right] \times W_i(R_i)\mathrm{d}R_i, \quad (4)$$

where $W_i(R_i)\mathrm{d}R_i$ is the probability of finding the $i$th acceptor at the distance between $R$ and $R+\mathrm{d}R$ from the donor. Since the donors and acceptors are assumed to be randomly distributed over the corresponding planes, the functions $W_i(R_i)$ are identical for all $i$, i.e. $W_i(R_i)=W(R)$. However, for the donor planes confined to the opposite membrane sides the probability functions should be normalized differently:

$$W_1(R)\mathrm{d}R = \frac{2R\mathrm{d}R}{R_d^2-(d_c-0.5d_t)^2} \quad \text{and}$$

$$W_2(R')\mathrm{d}R' = \frac{2R'\mathrm{d}R'}{R_d^2-(d_c+0.5d_t)^2}, \quad (5)$$

where $W_1(R)\mathrm{d}R$ stands for a donor localized in the acceptor-containing bilayer leaflet (i.e. in the upper donor plane in Fig. 1), and $W_2(R')\mathrm{d}R'$—for a donor residing in the opposite leaflet; $d_t$ is the distance between the two donor planes, and $d_c$ is the distance between the acceptor plane and the bilayer center.

Finally, the relative quantum yield of the donor, which is directly measurable in the steady-state RET experiment, is related to the average fluorescence decay function $\langle P(t)\rangle$ by the following expression:

$$Q_r = \frac{Q_{DA}}{Q_D} = \frac{\int_0^{\infty}\langle P(t)\rangle\mathrm{d}t}{\int_0^{\infty}\exp(-t/\tau_D)\mathrm{d}t}, \quad (6)$$

where $Q_D$ and $Q_{DA}$ are the donor quantum yields in the absence and presence of acceptor, respectively. By combining Eqs. (4)–(6), introducing the dimensionless time $\lambda = t/\tau_D$, and assuming that the donor partitions equally between the outer and inner membrane leaflets, one obtains:

$$Q_r = \frac{1}{2}\int_0^{\infty} e^{-\lambda}\left[(I_1(\lambda))^{N_1}+(I_2(\lambda))^{N_2}\right]\mathrm{d}\lambda, \quad (7)$$

where

$$I_1(\lambda) = \int_{|d_c-0.5d_t|}^{R_d}\exp\left[-\lambda\left(R_0/R\right)^6\right]W_1(R)\mathrm{d}R,$$

$$I_2(\lambda) = \int_{d_c+0.5d_t}^{R_d}\exp[-\lambda(R_0/R)^6]W_2(R)\mathrm{d}R \quad (8)$$

and $N_1$, $N_2$ are the numbers of acceptor molecules within the distance $R_d$ from the donor located either in the upper or lower bilayer leaflet, respectively; these quantities are related to the acceptor surface concentration $C_A^s$:

$$N_1 = \pi C_A^s[R_d^2-(d_c-0.5d_t)^2]; \quad N$$
$$N_2 = \pi C_A^s[R_d^2-(d_c+0.5d_t)^2], \quad (9)$$

$$C_A^s = \frac{B}{L\sum f_j S_j}, \quad (10)$$

$B$ being the molar concentration of bound acceptor, $L$ is the total lipid concentration, $f_j$ and $S_j$ are mole fraction and mean area per molecule, respectively, of the $j$th lipid species constituting the membrane.

### 2.2. Orientation factor problem

Under given conditions (polarity, degree of motional freedom, anisotropy of chromophore microenvironment) any donor–acceptor pair is characterized by a certain distance $R_0$ at which the rate constant of energy transfer $k_T$ is equal to the rate of the donor fluorescence decay $\tau_D^{-1}$ in the absence of acceptor [10]. According to Förster's theory this parameter (Förster radius) is related to spectral characteristics of the donor and acceptor as follows:

$$R_0^6 = \frac{9000(\ln 10)\kappa^2 Q_D J}{128\pi^5 n^4 N_A},$$

$$J = \frac{\int_0^{\infty} F_D(\nu)\varepsilon_A(\nu)\nu^{-4}\mathrm{d}\nu}{\int_0^{\infty} F_D(\nu)\mathrm{d}\nu} \quad (11)$$

where $\kappa^2$ is the orientation factor, $J$ is the spectral overlap integral, $F_D(\nu)$ is the donor emission

spectrum, $\varepsilon_A(\nu)$ is the acceptor absorbance spectrum, $n$ is the refractive index of the medium, and $N_A$ is Avogadro's number.

The orientation factor, characterizing the relative spatial orientation of the donor and acceptor transition dipoles, is given by

$$\kappa^2 = (\cos\theta_T - 3\cos\theta_D\cos\theta_A)^2, \quad (12)$$

where $\theta_T$ is the angle between the emission transition moment of the donor **D** and the absorption transition moment of the acceptor **A**, $\theta_D$ and $\theta_A$ are the angles between these moments and vector **R** joining the donor and acceptor. The angle $\theta_T$ can be further expressed in terms of the dihedral angle $\phi$ between the planes (**D**, **R**) and (**A**, **R**):

$$\cos\theta_T = \sin\theta_D\sin\theta_A\cos\phi + \cos\theta_D\cos\theta_A, \quad (13)$$

then

$$\kappa^2 = (\sin\theta_D\sin\theta_A\cos\phi - 2\cos\theta_D\cos\theta_A)^2. \quad (14)$$

As follows from Eq. (12), orientation factor can attain any value between 0 and 4, the minimum value corresponding to perpendicularly oriented donor and acceptor dipoles and the maximum one characterizing the case when these dipoles are parallel and identically directed. Due to considerable complications in experimental or theoretical evaluation of orientation factor it is a common practice in the RET studies to put $\kappa^2$ to be equal to 0.67. This value is valid for the isotropic and dynamic averaging conditions, when the donor and acceptor dipoles can adopt all orientations (isotropic condition) in a time short compared with the transfer time (dynamic averaging condition).

Eqs. (12)–(14) hold for the donor and acceptor whose transition moments do not experience any reorientations during the transfer time. Alternatively, for the rapidly tumbling donors and acceptors the dynamic average value of orientation factor ($\langle\kappa^2\rangle$) should be introduced. The formalism for obtaining this value has been described in detail in the early work of Dale et al. [30]. On the assumption of the limited orientational freedom of donors and acceptors it has been postulated that **D** and **A** exhibit random reorientation within cones about certain axes $\mathbf{D}_x$ and $\mathbf{A}_x$ (fixed with respect to the intramolecular coordinate system) in a time shorter than transfer time ('wobbling in cone' model). In this case the chromophore orientation can be described in terms of three angular parameters—$\theta_{D,A}$, the cone half-angles $\psi_{D,A}$, and the azimuthal angles $\gamma_{D,A}$ (Fig. 2), related by the following expressions:

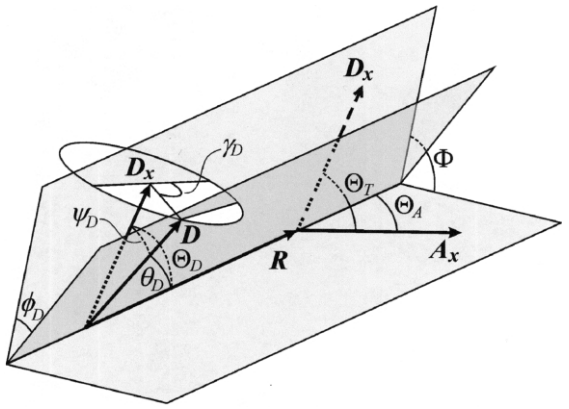


Fig. 2. The angles introduced by Dale et al. [30] in obtaining the dynamic average value of orientation factor (Eqs. (21) and (22)).

$$\phi = \Phi + \phi_A - \phi_D, \quad (15)$$

$$\sin\theta_{D,A}\sin\phi_{D,A} = \sin\psi_{D,A}\sin\gamma_{D,A}, \quad (16)$$

$$\cos\theta_{D,A} = \cos\Theta_{D,A}\cos\psi_{D,A} + \sin\Theta_{D,A}\sin\psi_{D,A}\cos\gamma_{D,A}, \quad (17)$$

$$\sin\theta_{D,A}\cos\phi_{D,A} = \sin\Theta_{D,A}\cos\psi_{D,A} - \cos\Theta_{D,A}\sin\psi_{D,A}\cos\gamma_{D,A}. \quad (18)$$

Combining Eqs. (15)–(18) with Eq. (14) and averaging over the azimuthal angles $\gamma_{D,A}$ with

$$\langle\cos\gamma_{D,A}\rangle = \langle\sin\gamma_{D,A}\rangle = \langle\cos\gamma_{D,A}\sin\gamma_{D,A}\rangle = 0, \quad (19)$$

$$\langle\cos^2\gamma_{D,A}\rangle = \langle\sin^2\gamma_{D,A}\rangle = 1/2 \quad (20)$$

permit the dynamic average $\kappa^2$ value to be derived:

$$\langle\kappa^2\rangle = \kappa^{x2}\langle d_D^x\rangle\langle d_A^x\rangle + 1/3(1-\langle d_D^x\rangle) + 1/3(1-\langle d_A^x\rangle) + \cos^2\Theta_D\langle d_D^x\rangle(1-\langle d_A^x\rangle) + \cos^2\Theta_A\langle d_A^x\rangle(1-\langle d_D^x\rangle), \quad (21)$$

in which

$$\kappa^{x2} = (\sin\Theta_D\sin\Theta_A\cos\Phi - 2\cos\Theta_D\cos\Theta_A)^2 \quad (22)$$

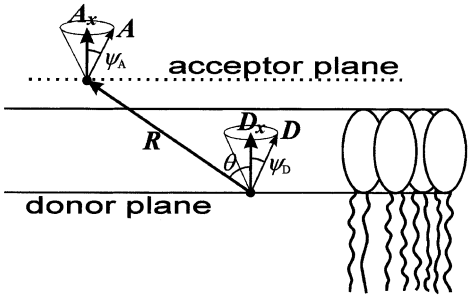


Fig. 3. Wobbling in cone model applied to membrane probes. Transition moment vectors of a donor (**D**) and an acceptor (**A**) have axially symmetrical distributions about their mean orientations $\mathbf{D}_x$ and $\mathbf{A}_x$, respectively.

is the axial orientation factor defined for the axial (mean) orientations $\mathbf{D}_x$ and $\mathbf{A}_x$ while $\langle d_{\mathrm{D}}^{\mathrm{x}}\rangle$ and $\langle d_{\mathrm{A}}^{\mathrm{x}}\rangle$ (also referenced as $d_{\mathrm{D}}$ and $d_{\mathrm{A}}$ below) are so-called axial depolarization factors

$$\langle d_{\mathrm{D,A}}^{\mathrm{x}}\rangle = 3/2\langle\cos^2\psi_{\mathrm{D,A}}\rangle - 1/2, \tag{23}$$

related to the steady state $r$ and fundamental $r_0$ anisotropies of donor and acceptor [30]:

$$d_{\mathrm{D,A}}^{\mathrm{x}} = \pm(r_{\mathrm{D,A}}/r_{0\mathrm{D,A}})^{1/2}. \tag{24}$$

Intramolecular energy transfer commonly occurs between the donor and acceptor attached to the substrate molecule in a unique way, so that every donor–acceptor pair in the sample appears to be placed in the same conditions. However, this is not the case for the donors and acceptors located in membrane where RET exhibits several peculiarities. First, there is no fixed distance between donors and acceptors but certain distribution of distances (Eq. (5)). Second, if the characteristic times of the chromophore rotational diffusion in fluid membrane are much shorter than the donor lifetime in the presence of acceptors, $\mathbf{D}_x$ and $\mathbf{A}_x$ should be parallel to the bilayer normal (Fig. 3). Indeed, since the membrane (modeled as an infinite plane) has a trivial axial symmetry with its normal being the symmetry axis, on the time scales much greater than the rotational diffusion rate the orientations of chromophore molecule will be mainly distributed symmetrically about the bilayer normal [34]. Third, for a given donor-acceptor pair the angles $\Theta_{\mathrm{D}}$ and $\Theta_{\mathrm{A}}$ formed by $\mathbf{D}_x$ and $\mathbf{A}_x$ with **R** are equal and depend on D–A separation (Figs. 2 and 3):

$$\Theta_{\mathrm{A}} = \Theta_{\mathrm{D}} = \theta, \quad \theta = f(R). \tag{25}$$

Taking into account the above rationales Eq. (21) can be rewritten as [31]:

$$\begin{aligned}\langle\kappa^2(\theta)\rangle = {} & \langle d_{\mathrm{D}}^{\mathrm{x}}\rangle\langle d_{\mathrm{A}}^{\mathrm{x}}\rangle(3\cos^2\theta - 1)^2 + 1/3(1 - \langle d_{\mathrm{D}}^{\mathrm{x}}\rangle) \\ & + 1/3(1 - \langle d_{\mathrm{A}}^{\mathrm{x}}\rangle) + \cos^2\theta \\ & \times\left(\langle d_{\mathrm{D}}^{\mathrm{x}}\rangle - 2\langle d_{\mathrm{D}}^{\mathrm{x}}\rangle\langle d_{\mathrm{A}}^{\mathrm{x}}\rangle + \langle d_{\mathrm{A}}^{\mathrm{x}}\rangle\right).\end{aligned} \tag{26}$$

Thus, orientation factor appears to be a function of the angle $\theta$ and, therefore, of $R$, since

$$\cos^2\theta = \left(\frac{d_{\mathrm{c}} \mp 0.5 d_{\mathrm{t}}}{R}\right)^2, \tag{27}$$

in which signs '−' and '+' correspond to the donor located in the upper or lower plane, respectively. Typical dependencies of (dynamic) average orientation factor on the donor–acceptor separation or, equivalently, on θ are shown in Fig. 4. It should be noted that these functions are mainly non-monotonic, 'crinkling' about their respective mean values lying between ~0.5 and ~1.5. Furthermore, as will be discussed below, almost all the

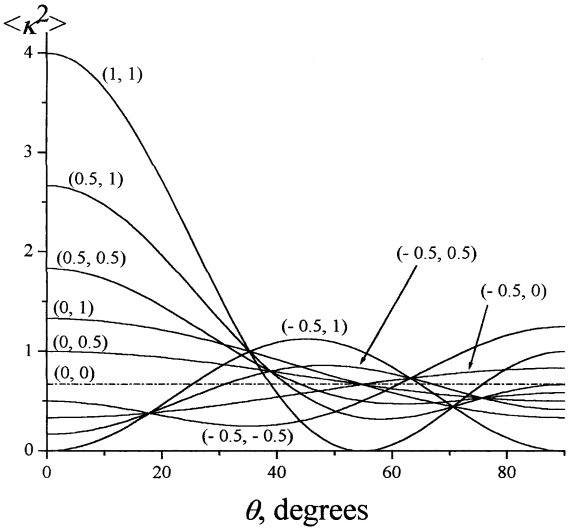


Fig. 4. Dependencies of dynamically averaged orientation factor on the angle θ between the bilayer normal and vector $\mathbf{R}_i$ joining donor and acceptor. Pairs of axial depolarization factors ($d_{\mathrm{A}}$,$d_{\mathrm{D}}$) used in $\langle\kappa^2(\theta)\rangle$ calculation are shown in parentheses next to the curves. Straight heavy dash-dot line corresponds to $d_{\mathrm{D}} = d_{\mathrm{A}} = 0$.

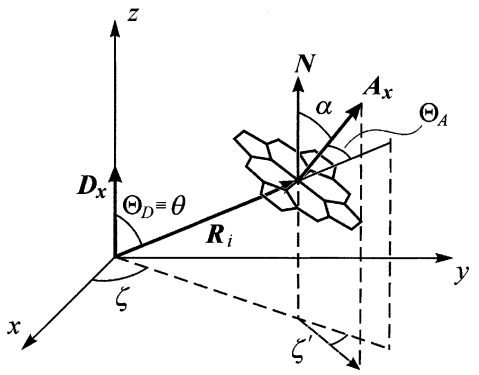


Fig. 5. The angular relationships corresponding to the case when symmetry axis of donor reorientation $\mathbf{D}_x$ is parallel to bilayer normal *N*, while the acceptor transition moment is distributed about normal to the plane making angle α with the membrane surface. ζ and ζ′ are azimuthal angles defining the orientation of transfer vector $\mathbf{R}_i$ and $\mathbf{A}_x$, respectively.

values of $\kappa^2$ corresponding to $0 \leqslant \theta < \pi/2$ contribute to the overall energy transfer since for the most cases in practice arccos $|(d_c \pm 0.5d_t)/R_d|$ is close to $\pi/2$.

Thus Eq. (8) can be modified to adopt the distance-dependent orientation factor $\langle\kappa^2(R)\rangle$:

$$I_{1,2}(\lambda) = \int_{|d_c \mp 0.5d_t|}^{R_d} \exp\left[-\lambda\kappa^2(R)\left(\frac{R_0^r}{R}\right)^6\right] \times \left(\frac{2R}{R_d^2 - (d_c \mp 0.5d_t)^2}\right) dR, \quad (28)$$

here Förster radius is represented as $R_0^6 = \kappa^2(R)\cdot(R_0^r)^6$, $R_0^r = 979(n_r^{-4}Q_D J)^{1/6}$ (cf., Eq. (11)).

All the above considerations provide a theoretical background for analyzing one particular case of interest when energy transfer takes place between membrane-incorporated fluorescent probe as a donor and the protein chromophore (e.g. heme or covalently attached label) as an acceptor [22,35]. Assuming that the protein has certain specific orientation with respect to the bilayer, the general model presented above can be easily extended to describe such situation. In this case the axis of acceptor distribution $\mathbf{A}_x$, being perpendicular to the plane of the protein chromophore, makes an angle *a* with the bilayer normal **N** (Fig. 5). The azimuth ζ′ describes the protein rotation about the bilayer normal **N**, whereas the azimuth ζ characterizes the direction from the donor toward a given acceptor and therefore it will be different for different acceptors surrounding the donor. Using the averaging procedure proposed by Dale et al. [30] it can be shown that in this case the dynamic average value of the orientation factor is also described by Eqs. (24) and (25) provided that the following substitution is made:

$$\langle d_A^x \rangle = \langle d_A^0 \rangle \cdot \left(\frac{3}{2}\cos^2\alpha - \frac{1}{2}\right). \quad (29)$$

Here $\langle d_A^0 \rangle$ stands for the axial depolarization factor associated with intramolecular reorientations about $\mathbf{A}_x$ while the term $(3/2\cos^2\alpha - 1/2)$ represents the additional depolarization factor due to $\mathbf{A}_x$ deviation from the membrane normal. Particularly, in the case of heme acceptor, which is commonly treated as a planar oscillator [33], $\langle d_A^0 \rangle$ equals $-1/2$ since $\psi_A = \pi/2$. In the averaging procedure the following relationships were utilized in addition to Eqs. (15)–(18) (Fig. 5):

$$\cos\Theta_A = \cos\alpha\cos\Theta_D + \sin\alpha\sin\Theta_D\cos\zeta', \quad (30)$$

$$\cos\alpha = \cos\Theta_A\cos\Theta_D + \sin\Theta_A\sin\Theta_D\cos\Phi. \quad (31)$$

The initial expression Eq. (14) was averaged over $\gamma_D$, $\gamma_A$, and ζ′ using the identities ([19,20]) together with the equivalent expressions for ζ′. Alternatively, Eq. (29) can be obtained by direct application of Soleillet's theorem, stating the multiplicativity of independent depolarization factors.

It should also be noted that the above derivation has been performed in the dynamic averaging limit, thus implying that the rotational diffusion of the membrane-bound protein (the acceptor) is much faster than the energy transfer. Otherwise, the orientation factor will also depend on the azimuth ζ′ between the planes (**N**, $\mathbf{A}_x$) and (**N**, **R**):

$$\langle\kappa^2\rangle = f(R,\alpha,\zeta'). \quad (32)$$

The exact expression for $\langle\kappa^2(R,\alpha,\zeta')\rangle$ can be obtained by substituting

$$\kappa^{x2} = (\cos\alpha - 3\cos\Theta_D\cos\Theta_A)^2 \quad (33)$$

into Eq. (21) and then expanding $\cos\Theta_A$ according to Eq. (30). In order to average $\kappa^2$ in this case

Eq. (28) should be rewritten as:

$$I_{1,2}(\lambda)=\int_{|d_c\mp 0.5d_t|}^{R_d}\int_0^{2\pi}\exp\left[-\lambda\kappa^2(R,\alpha,\zeta')\times\left(\frac{R_0^r}{R}\right)^6\right]\cdot W_{1,2}(R)\,d\zeta'\,dR. \quad (34)$$

Application of this model to analyzing the experimental data requires the following experimental tasks to be performed: (1) determination of the donor quantum yield in the membrane environment, needed for the calculation of $R_0^r$; (2) estimation of bound acceptor surface concentration; (3) measuring the relative quantum yield $Q_r$ as a function of the acceptor concentration $C_A^s$, and; if possible, (4) evaluating the donor and acceptor depolarization factors. Finally, the structural parameter $d_c$ can be derived by least square fitting of the theoretical curves calculated using appropriate model parameters to the measured dependencies $Q_r(C_A^s)$.

## 3. Results

Shown in Fig. 6 are the quenching profiles illustrating the dependence of RET efficiency or, equivalently, relative quantum yield of the donor on the acceptor distance from the bilayer center. These profiles were obtained by numerical integration of Eqs. (7)–(10) assuming that both isotropic and dynamic averaging conditions are satisfied (i.e. $\kappa^2=0.67$) and varying $d_c/R_0$ ratio from 0 to 2. Increasing this ratio results in the lowered RET efficiency with $Q_r$ values being rather insensitive to variations in the distance between the two donor planes $d_t$.

Next, it seems of significance to assess how considering $\kappa^2$ as a function of the donor–acceptor distance (or angle $\theta$) and depolarization factors $d_D$ and $d_A$ rather than a parameter attaining unique value, would affect the $Q_r(d_c)$ dependencies. Presented in Fig. 7 are the sets of $Q_r$ vs. $d_c$ plots (dotted lines) calculated allowing $d_D$ and $d_A$ to vary over the widest possible limits (from $-0.5$ to 1.0). By excluding unrealistic cases of considerably immobilized donors and acceptors where $d_D$ and $d_A$ are close to unity, these curves are seen to be confined to a certain region restricted by the

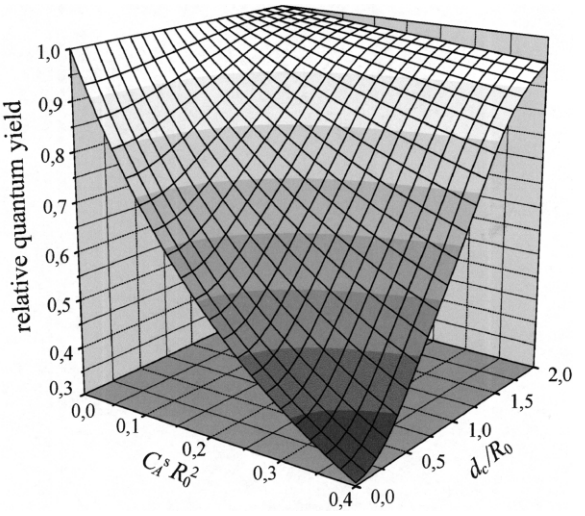


Fig. 6. Dependence of relative quantum yield of the donor $Q_r$ on the dimensionless acceptor (surface) concentration $C_A^s R_0^2$ and dimensionless acceptor plane separation from the bilayer center $d_c/R_0$ calculated numerically according to the present model in the limit of both isotropic and dynamic averaging (i.e. $d_D=d_A=0$, $\kappa^2=0.67$, $R_0=$const). The distance between the two donor planes was $0.8R_0$.

upper and lower envelopes (heavy solid lines) corresponding to the maximum and minimum $Q_r$ values derived for given acceptor surface concentration and the distance between donor arrays. Importantly, the average width of such region, reflecting the proximity of the $Q_r(d_c)$ plots, is characterized by a clear dependence on the separation of the donor planes (different panels in Fig. 7). Comparison of these plots shows that, for a particular case of $R_0=3.0$ nm, the narrowest $Q_r$ limits are observed at $d_t\sim 2$–$2.4$ nm. This finding made us assume that there exist certain $d_t/R_0$ limits in which $Q_r(d_c)$ plots exhibit the closest proximity, thus allowing one to minimize the error in $d_c$ estimation resulting from taking the isotropic $\kappa^2$ value (0.67) instead of using experimentally measured $d_D$ and $d_A$ parameters.

In view of this the following step of numerical simulation was aimed at recovering the dependence of the accuracy of $d_c$ estimation ($\Delta d_c/R_0$) on such parameters as $d_t/R_0$ and $d_c/R_0$. Note that in obtaining simulation results we mainly utilized the dimensionless separations $d_t/R_0$ and $d_c/R_0$ as well

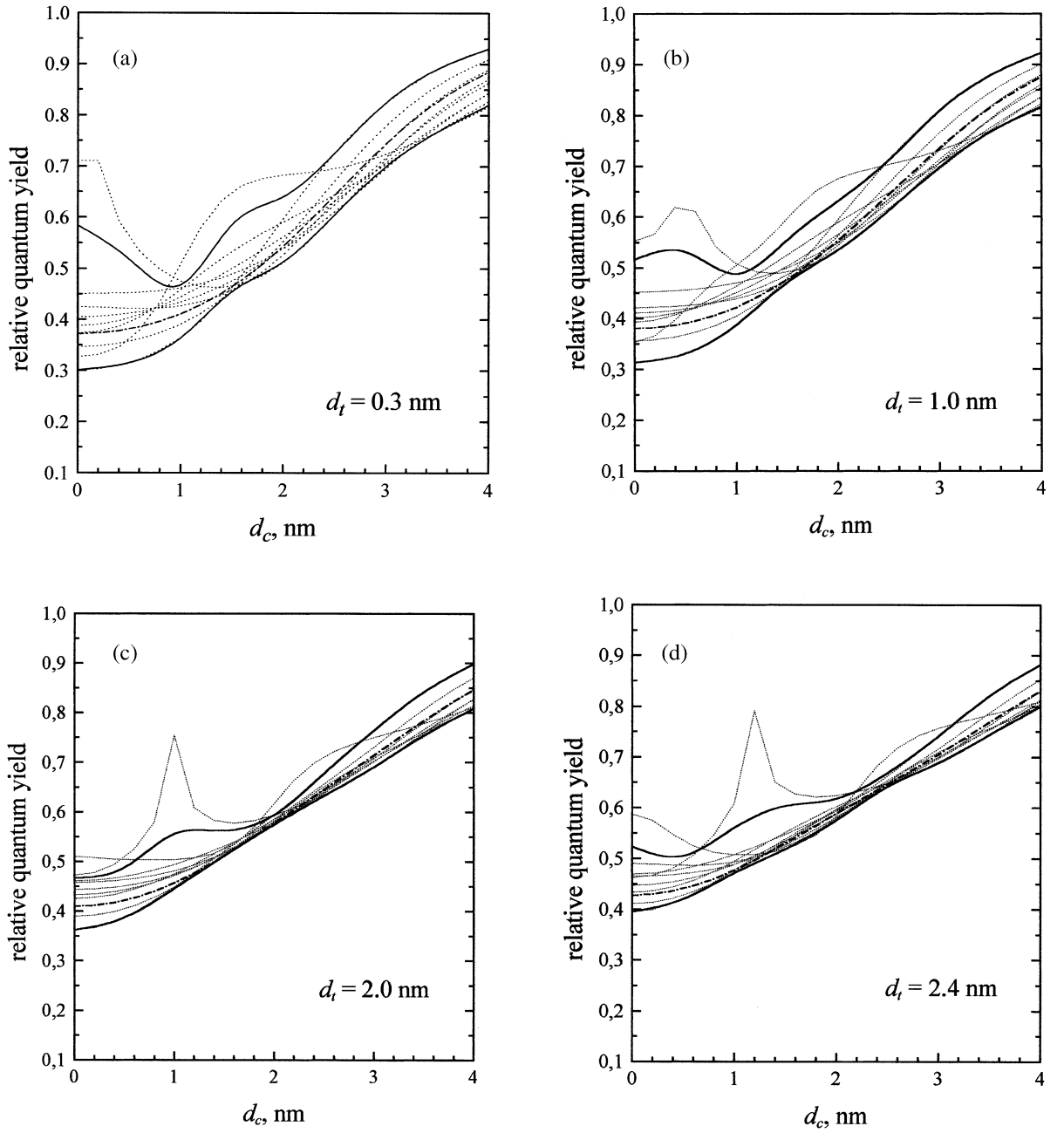


Fig. 7. Relative quantum yield of the donor $Q_r$ as a function of the acceptor plane separation from the bilayer center $d_c$ (dotted lines) calculated for different parameter sets. The acceptor surface concentration was kept constant ($C_A^s = 0.03$ nm$^{-2}$), and $R_0^r$ was chosen to be $3/\sqrt[3]{0.67} \cong 3.2$nm. The distance between the two donor planes $d_t$ was varied from 0.3 to 4.0 nm (panels A to F). Each set of curves was obtained by varying the depolarization factors $d_D$ and $d_A$ from $-0.5$ to 1. Shown with heavy solid lines are the envelopes to the sets of curves, representing the bounds of $Q_r$ uncertainty due to unknown $d_D$ and $d_A$ at a given $d_c$. Note that for calculation of the envelopes the ranges $-0.5 \div 0.9$ for $d_D$ and $d_A$ were used. The curves corresponding to $\kappa^2 = 0.67$ are stressed (heavy dash-dot lines).

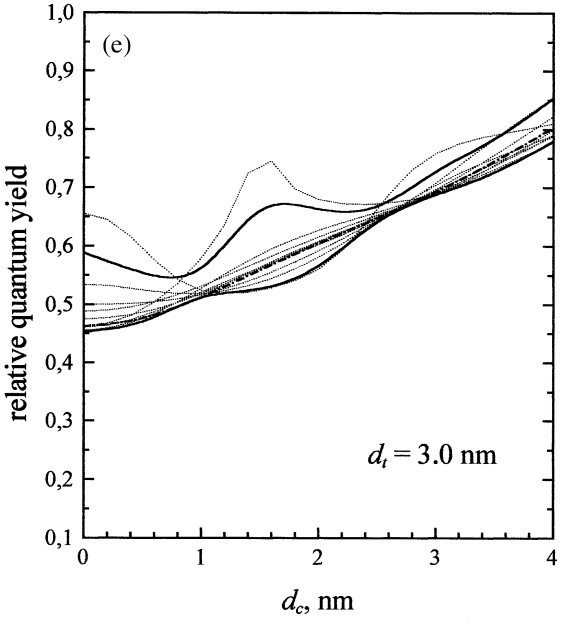


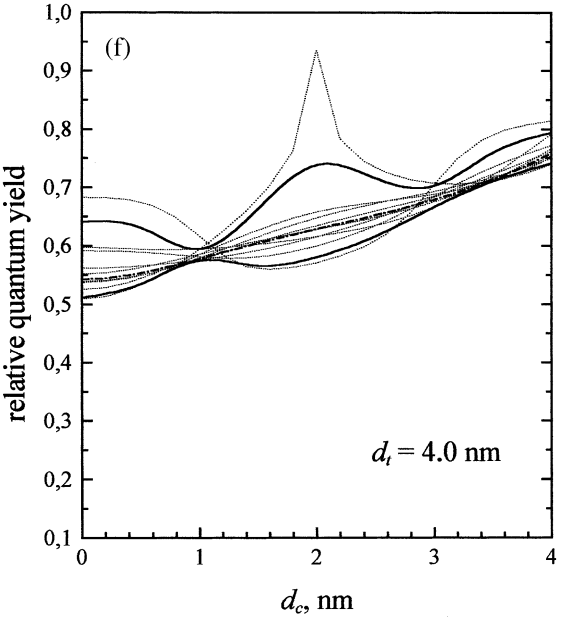


Fig. 7 (Continued).

as dimensionless surface concentration $C = C_A^s R_0^2$ to make the model independent of $R_0$ and, therefore, to generalize the analysis for any pair of chromophores characterized by specific $R_0$. Analysis of the results presented in Fig. 8 shows that in certain area corresponding to $d_t/R_0$ and $d_c/R_0$

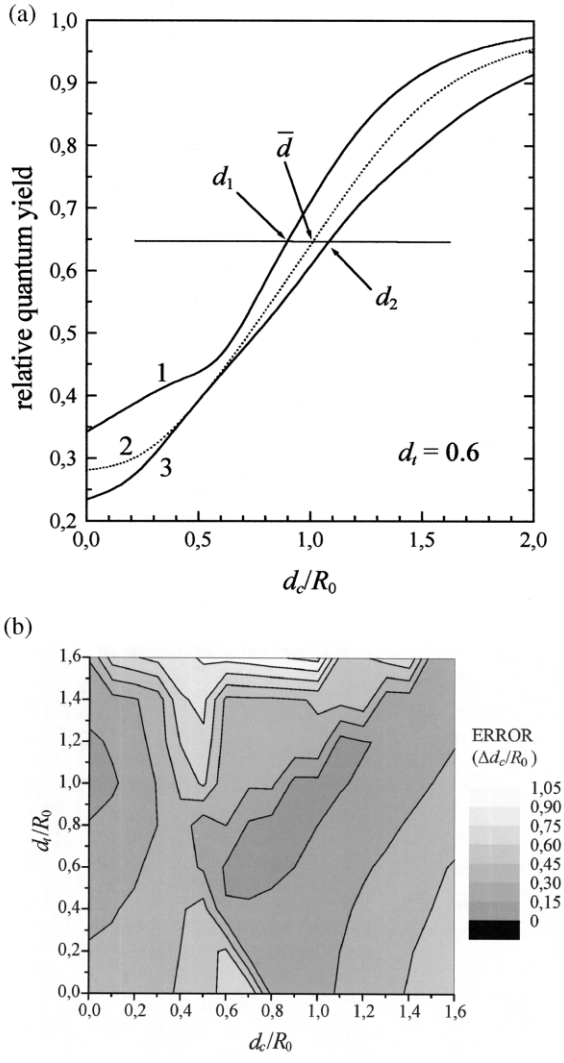


Fig. 8. (A) Typical graph used for obtaining the error of $d_c$ estimation ($\Delta d_c$) as a function of $d_t$ and $d_c$. The upper and lower curves restrict the range of $Q_r$ values calculated with $d_D$ and $d_A$ varying from $-0.5$ to 0.9, while the dotted curve corresponds to $\kappa^2 = 0.67$. Intercepts of horizontal lines with curves 1, 2, 3 yield the $d_c$ values $d_1$, $\bar{d}$, $d_2$ that were used subsequently to calculate $\Delta d_c = f(\bar{d}) = d_2 - d_1$. All distances (including $\Delta d_c$) are expressed in $R_0$ units; (B) Contour plot for $d_t$ and $d_c$ sets corresponding to different errors in $\Delta d_c$ estimation. Acceptor concentration $C_A^s R_0^2 = 0.4$.

values lying between approximately 0.6–1.2 the error in $d_c$ estimation is characterized by a clear minimum.

## 4. Discussion

In analyzing the above simulation results it seems of significance to point out several essential aspects of energy transfer in membranes. The first aspect concerns the contribution of orientational effects to the RET efficiency. In the case of intramolecular energy transfer each donor–acceptor pair is characterized by a certain dynamic average orientation factor. A different situation occurs in the systems where donors and acceptors are distributed over separate planes and energy is transferred from a donor to an ensemble of acceptors. As illustrated in Fig. 4, in this case $\kappa^2$ shows explicit dependence on the angle between the bilayer normal $N$ and the transfer vector $\mathbf{R}$, i.e. $\kappa^2$ values will be distinct for the acceptors residing at different distances from a donor. One consequence of this fact involves rather low sensitivity of the relative quantum yield of a donor to the degree of the chromophore rotational freedom. For instance, as can be seen in Fig. 7, varying the $d_D$ and $d_A$ values in the widest realistic limits ($-0.5$ to 0.9) results in the $Q_r$ changes not exceeding 0.3 in the worst case of $d_t = d_c = 0$ (all donors and acceptors are confined to the same plane). From mathematical point of view this fact could be explained in the following manner. Since the $\kappa^2(\theta)$ dependencies are non-monotonic (Fig. 4), the contributions from the $\kappa^2$ values being higher and lower than 0.67 to some extent compensate each other thus causing the calculated quenching profiles to approach $Q_r$ value corresponding to isotropic conditions ($\kappa^2 = 0.67$). Interestingly, this fact manifests itself in Fig. 7. Indeed, in each plot one can see a region around $d_c = d_t/2$ showing enhanced dependence of RET efficiency on $d_D$ and $d_A$, which results from the elimination of orientation factor dependence (Eq. (27)) on D–A separation for one of the donor planes (in this case the donor plane coincides with the acceptor plane and $\theta = \text{constant} = \pi/2$).

The second aspect of the problem being scrutinized concerns the errors in the quantitative interpretation of RET data, stemming from the common practice of taking $\kappa^2 = 0.67$. In this context it is reasonable to distinguish the errors introduced by the non-ideality of experimental procedure and those associated with uncertainty in the parameters of theoretical model employed. The reliability of steady state experimental data is determined by the accuracy of fluorescence intensity measurements, which reaches $\pm 3-5\%$ in the most well-designed experiments [10], as well as by the error in the estimation of acceptor surface concentration. On the other hand, the most widely discussed drawback of RET models is the uncertainty in the relative orientation of the donor and acceptor transition moments and, consequently, in the orientation factor. The results presented here (Fig. 7) show that in membrane systems there exist certain combinations of parameters $d_t/R_0$ and $d_c/R_0$ at which the uncertainty introduced by the model (when the donor and acceptor axial depolarization factors are allowed to take any value in the range from $-0.5$ to 0.9) is less or comparable with the minimum experimental error.

The third important aspect concerns the possibility of minimizing the uncertainty in estimating the acceptor membrane location by choosing the most appropriate donors. As follows from the results presented in Fig. 8, the maximum accuracy of $d_c$ evaluation could be achieved when the acceptor distance from the bilayer center is close to the separation of the donor planes ($d_c - d_t$) and $d_t$ to $R_0$ ratio lies between 0.6 and 1.2. Given that for the most donor–acceptor pairs employed in the membrane studies $R_0$ falls in the range 2–4 nm [11], the latter condition implies that membrane location of the acceptor whose $d_c$ is less than 1.2 nm could not be evaluated with desirable confidence. If it is necessary to ascertain the bilayer position of a given acceptor the donors employed are required to be: (i) uniformly distributed between the outer and inner membrane leaflets; (ii) confined to the parallel planes with known separation; (iii) characterized by $d_t/R_0$ values lying between 0.6 and 1.2. The first requirement is supported by the data shown in Fig. 8, indicating that as $d_t/R_0$ value approaches zero the errors in $d_c$ estimation significantly increase. It is also noteworthy that using the donors distributed between

the outside and inside of the bilayer permits the acceptor distance from membrane center to be evaluated unequivocally, while in the case of the donors restricted to one monolayer additional information as to the side of the donor array facing the acceptors is needed.

In conclusion, it seems of importance to draw attention to several principal issues concerning the application of RET method in recovering the proximity relation in membranes. In two-dimensional systems containing donors and acceptors confined to separate planes the contribution of orientational effects to energy transfer efficiency proved to be substantially lower than that observed in the case of intramolecular RET. This essential feature of RET in membrane originates from the involvement of a number of acceptors in the energy transfer from a given donor and varying the orientation factor value with the donor–acceptor distance. Peculiar orientational dependence of membrane RET appears to be conductive to the existence of experimental conditions under which the error in distance estimation resulting from the unknown depolarization factors of chromophores and using the isotropic $\kappa^2$ value would be minimum.

The RET model presented here is valid for a particular case of two donor planes separated by a fixed distance and one acceptor plane. The aforementioned theoretical approaches and practical recommendations may prove of usefulness in elucidating the acceptor location in the systems with such chromophore distribution.

## Acknowledgments

We are very grateful to Drs P.W. Holloway, J. Eisinger, and M.F. Brown for providing us with the reprints of papers.

## References

[1] M. Garavito, S. White, Membrane proteins. Structure, assembly and function: a panoply of progress, Curr. Opin. Struct. Biol. 7 (1997) 533–536.

[2] M. Sabra, O. Mouritsen, Steady-state compartmentalization of lipid membranes by active proteins, Biophys. J. 74 (1998) 745–752.

[3] M. Wiener, S. White, Structure of a fluid dioleoylphosphatidylcholine bilayer determined by joint refinement of X-ray and neutron diffraction data, Biophys. J. 61 (1992) 434–447.

[4] K. Hristova, W. Wimley, V. Mishra, G. Anantharamaiah, J. Segrest, S. White, An amphipathic α-helix at a membrane interface: a structural study using a novel X-ray diffraction method, J. Mol. Biol. 290 (1999) 99–117.

[5] T. Heimburg, P. Hildebrandt, D. Marsh, Cytochrome c-lipid interactions studied by resonance Raman and $^{31}$P NMR spectroscopy. Correlation between the conformational changes of the protein and lipid bilayer, Biochemistry 30 (1991) 9084–9089.

[6] P.J.R. Spooner, A. Watts, Reversible unfolding of cytochrome *c* upon interaction with cardiolipin bilayers. 1. Evidence from deuterium NMR measurements, Biochemistry 30 (1991) 3871–3879.

[7] C. Dempsey, Amide-resolved hydrogen–deuterium exchange measurements from membrane-reconstituted polypeptides using exchange trapping and semiselective two-dimensional NMR, J. Biomol. NMR 4 (1994) 879–884.

[8] H.I. Petrache, S.W. Dodd, M.F. Brown, Area per lipid and acyl length distributions in fluid phosphatidylcholines determined by $^{2}$H NMR spectroscopy, Biophys. J. 79 (2000) 3172–3192.

[9] D. Marsh, ESR spin-label study of lipid-protein interactions, Progr. Protein-Lipid Interact. Amsterdam, 1985, pp. 143–172.

[10] J.R. Lakowicz, Principles of Fluorescent Spectroscopy, Plenum Press, New York, 1999.

[11] P. Wu, L. Brand, Resonance energy transfer: methods and applications, Anal. Biochem. 218 (1994) 1–13.

[12] J. Matko, M. Edidin, Energy transfer methods in detecting molecular clusters on cell surfaces, Meth. Enzymol. 278 (1997) 444–462.

[13] M. Rytömaa, P.K.J. Kinnunen, Evidence for two distinct acidic phospholipid-binding sites in cytochrome *c*, J. Biol. Chem. 269 (1994) 1770–1774.

[14] P. Bastiaens, A. de Beus, M. Lacker, P. Somerharju, M. Vauhkonen, J. Eisinger, Resonance energy transfer from a cylindrical distribution of donors to a plane of acceptors. Location of apo-B100 protein on the human low-density lipoprotein particle, Biophys. J. 58 (1990) 665–675.

[15] R. Doebler, N. Başaran, H. Goldston, P.W. Holloway, Effect of protein aggregation in the aqueous phase on the binding of membrane proteins to membranes, Biophys. J. 76 (1999) 928–936.

[16] J. Ren, S. Lew, Z. Wang, E. London, Transmembrane orientation of hydrophobic α-helices is regulated both by the relationship of helix length to bilayer thickness and by the cholesterol concentration, Biochemistry 36 (1997) 10213–10220.

[17] J. Silvius, M. Zuckermann, Interbilayer transfer of phospholipid-anchored macromolecules via monomer diffusion, Biochemistry 32 (1993) 3153–3161.
[18] G. Gorbenko, Resonance energy transfer study of hemoglobin complexes with model phospholipid membranes, Biophys. Chem. 81 (1999) 93–105.
[19] P. Haris, D. Chapman, Structural studies of membrane associated polypeptides and proteins using Fourier transform infrared spectroscopy, Biochemistry 20 (1990) 49–60.
[20] A.S. Ladokhin, P.W. Holloway, E.G. Kostrzhevska, Distribution analysis of membrane penetration of proteins by depth-dependent fluorescence quenching, J. Fluorescence 3 (1993) 195–197.
[21] J. Eisinger, J. Flores, Cytosol-membrane interface of human erythrocytes. A resonance energy transfer study, Biophys. J. 41 (1983) 367–379.
[22] G. Gorbenko, Structure of cytochrome *c* complexes with phospholipids as revealed by resonance energy transfer, Biochim. Biophys. Acta 1420 (1999) 1–13.
[23] L.M.S. Loura, A. Fedorov, M. Prieto, Resonance energy transfer in a model system of membranes: application to gel and liquid crystalline phases, Biophys. J. 71 (1996) 1823–1836.
[24] B. Fung, L. Stryer, Surface density determination in membranes by fluorescence energy transfer, Biochemistry 17 (1978) 5241–5248.
[25] P. Wolber, B. Hudson, An analytic solution to the Forster energy transfer problem in two dimensions, Biophys. J. 28 (1979) 197–210.
[26] T. Estep, T. Thompson, Energy transfer in lipid bilayers, Biophys. J. 26 (1979) 195–208.
[27] T. Dewey, G. Hammes, Calculation of fluorescence resonance energy transfer on surfaces, Biophys. J. 32 (1980) 1023–1036.
[28] B. Snyder, E. Freire, Fluorescence energy transfer in two dimensions. A numeric solution for random and nonrandom distributions, Biophys. J. 40 (1982) 137–148.
[29] M. Doody, L. Sklar, H. Pownall, J. Sparrow, A. Gotto, L. Smith, A simplified approach to resonance energy transfer in membranes, lipoproteins and spatially restricted systems, Biophys. Chem. 17 (1983) 139–152.
[30] R. Dale, J. Eisinger, W. Blumberg, The orientational freedom of molecular probes. The orientation factor in intramolecular energy transfer, Biophys. J. 26 (1979) 161–194.
[31] L. Davenport, R. Dale, R. Bisby, R. Cundall, Transverse location of the fluorescent probe 1,6-diphenyl-1,3,5-hexatriene in model lipid bilayer membrane systems by resonance excitation energy transfer, Biochemistry 24 (1985) 4097–4108.
[32] P. Wu, L. Brand, Orientation factor in steady state and time-resolved resonance energy transfer measurements, Biochemistry 31 (1992) 7939–7947.
[33] Z. Gryczynski, T. Tenenholz, E. Bucci, Rates of energy transfer between tryptophans and hemes in hemoglobin, assuming that the heme is a planar oscillator, Biophys. J. 63 (1992) 648–653.
[34] M.L. Huertas, V. Cruz, J.J. López Cascales, A.U. Acuña, J. García de la Torre, Distribution and diffusivity of a hydrophobic probe molecule in the interior of a membrane: theory and simulation, Biophys. J. 71 (1996) 1428–1439.
[35] J. Eisinger, J. Flores, R.M. Bookchin, The cytosol-membrane interface of normal and sickle erythrocytes. Effect of hemoglobin deoxygenation and sickling, J. Biol. Chem. 259 (1984) 7169–7177.